Linear and Networked Blends and Copolymers of Polyimide

Jiqiang Xia,* Jinwei Wang,† M. P. Srinivasan

Department of Chemical and Biomolecular Engineering, National University of Singapore, Singapore 117576

Received 15 June 2004; accepted 5 May 2005
DOI 10.1002/app.22991
Published online in Wiley InterScience (www.interscience.wiley.com).

ABSTRACT: Preparation and characterization of blends and copolymers of a fluorinated polyimide with network constituents is reported. 4,4′-Hexafluoroisopropylidene diphthalic anhydride and 4,4′-diaminodiphenyl ether (6FDA–DDE) polyimide were used as the linear hosts and mellitic acid hexamethyl ester - 4,4′-diaminodiphenyl ether (MAHE–DDE) was employed as the network constituent for the blend and copolymer. Cast films of the polyimides were characterized by FTIR, XPS, DMA, and TGA. The multifunctional nature of MAHE facilitated crosslinking among the constituents. Both blends and copolymers showed significant improvement in the storage modulus and glass transition temperature relative to that observed for the 6FDA homopolymer. The occurrence of a single glass transition temperature for the blends suggests that they were at least partially miscible. Presence of low molecular weight species in the copolyimides, combined with steric hindrance to crosslinking, may have resulted in the existence of an optimum in the amount of the network components for improving the mechanical properties. Inclusion of network components is presented as a facile method for improving the desirable properties of polyimide. © 2006 Wiley Periodicals, Inc. J Appl Polym Sci 100: 3000–3008, 2006

Key words: polyimide; network; blend; crosslinking

INTRODUCTION

Aromatic polyimides (PI) have been widely used in industry as structural materials, as dielectric materials for insulators, etc. since they possess many useful properties.[1] For practical applications, a certain polyimide may achieve some of the required properties. Evidently, all the property requirements cannot easily be met by a single homopolyimide. Polymer blends and copolymers are relatively economical to produce and generally cause a lower technical risk than that involved in developing a new polymer or polymeric composition.[2] Accordingly, research in the area of polymeric blends, copolymers, composites, and interpenetrating network systems has been very intense. The value addition of commercial polymers (both commodity and specialty grades) and avenues for fundamental research in these emerging fields have culminated in tailoring of the properties of the polymers to meet very specific technological requirements. Processable aromatic polyimides were synthesized and the mechanical, melt-flow, and thermal properties have been studied.[3] Random and block copolyimides were synthesized based on pyromellitic dianhydride (PMDA), *p*-phenylene diamine (PDA) and 4,4′-diaminodiphenyl ether (DDE) and their mechanical properties were reported.[4] Yamamoto et al.[5] synthesized polyimide blends and copolyimides based on PMDA, PDA, and DDE and discussed the coefficient of thermal expansion (CTE) difference between polyimide blends and copolyimides. Several research groups[6–8] have reported the preparation of high-modulus, high-strength films with either homopolyimide or PI/PI blends (molecular composite) by thermal imidization of cold drawn poly(amic acid) (PAA) precursor films. Molecular composites have also been synthesized, such as 3,4,3′,4′-biphenyl tetracarboxylic dianhydride (BPDA)–PDA and PMDA–PDA (the rigid, reinforcing component) together with BPDA–DDE and PMDA–DDE (the flexible matrix).[9] Interpenetrating polymer network (IPN) polyimides were synthesized to develop tougher polymers that are more resistant to microcracking.[10] Takekoshi and Terry[11] studied several crosslinked polyimide systems to determine the reactivity and performance of disubstituted acetylenes used as curing end groups in high temperature composite matrix resins. Polybenzimidazole (PBI)/PI blends have been studied widely because of the theoretical and practical importance of these high performance polymers.[12] In summary, modification of polyimide properties through copolymer-

**Present address:* School of Materials Science and Engineering, Clemson University, USA.
†*Present address:* University of Science and Technology, Beijing, China.
Correspondence to: M. P. Srinivasan (chesmp@nus.edu.sg).
Contract grant sponsor: National University of Singapore.

ization and blending has been under extensive investigation in the last two decades and is still a topic of great interest.

Polyimides containing multifunctional reactants have not been investigated extensively so far, despite the potential for creating robust network structures. The preparation and properties of a mellitic acid-based polyimide were reported recently.[13] The preparation of mellitic acid hexamethyl ester (MAHE)-based polyimide blends and copolymers have been studied,[14,15] where the focus of the study was the processing conditions/parameters for imidization. To continue our efforts to improve the mechanical properties and stability of polyimide and further reveal the structure–property relationship, the MAHE-based polyimide blends and copolymers were studied in this work. The chemical composition of mellitic acid polymer (MAP) was analyzed and was followed by investigation of blending and copolyimide formation in 6FDA–DDE/MAP systems. The 6FDA–DDE polyimide system is of particular interest because of its highly desirable properties such as solubility, hydrophobicity, permeability, etc., and is a prime candidate for reinforcement because of its relatively weak thermal and mechanical properties.[16]

In this work, the mechanical and thermal properties are discussed in terms of network formation in the blends and copolymers. The presence of crosslinking agents (MAP and MAHE) improves the storage modulus and increases the glass transition temperature (T_g) of the material. Furthermore, at elevated temperatures, the rate of weight loss is lowered and the weight retention capability is improved because of the formation of networks.

EXPERIMENTAL

Materials

4,4′-(Hexafluoroisopropylidene)diphthalic anhydride (6FDA) from Aldrich was purified by sublimation at 240°C under vacuum followed by vacuum drying at 180°C for 4 h. 4,4′-Diaminodiphenyl ether (DDE) from Fluka was purified by recrystallization from ethanol followed by vacuum drying at 80°C for 4 h. Mellitic acid hexamethyl ester (MAHE) from TCI was used after vacuum drying at 120°C for 4 h.

Sample preparation

The linear polymer was prepared by dissolving DDE in *N*,*N*-dimethylacetamide (DMAc) followed by addition of 6FDA in stoichiometric amounts. The solution was stirred for 2 h at 25°C under a stream of nitrogen to obtain a lemon-yellow, viscous solution.

The mellitic acid polymer (MAP) precursor was prepared by dissolving DDE and MAHE in the molar ratio (DDE : MAHE) of 3 : 2 in DMAc. The monomer was added in the same manner as for making 6FDA–DDE. The solution was stirred for 2 h under a blanket of nitrogen while the temperature was raised from room temperature to a final value of approximately 135°C. A dark brown solution was obtained.[14]

To prepare the copolyimide precursor, DDE and MAHE were dissolved in DMAc as above and the solution was cooled in an ice bath to freezing point. The amount of MAHE in the solution was varied such that the network content ranged from 2 to 10%. 6FDA was added subsequently and the solution was stirred for 2 h in an ice bath to obtain the copolymer precursor solution.

The precursor solutions were cast as films in petri dishes. For the blends, the precursor solutions containing the linear and network constituents were mixed in different proportions in a flask stirred for 4 h and cast as films in petri dishes. The films were dried at 80°C in a vacuum oven for 2 h (prebaked) and stored in a desiccator. The dried samples were placed in a furnace and heated to 350°C in air for 90 min, with a ramp rate of 2°C min^{-1} (thermally treated). This finally resulted in the imidized blends (6FBL) and copolymers (6FCO). The materials are denoted by 6FBL-*x* and 6FCO-*x*, where '*x* ' refers to the MAP content by weight percent.

Schematic formulae of monomers used in this study and the poly(amic acid) formation formula are shown in Figure 1.

Characterization

Fourier transform Infrared (FTIR) spectra obtained for the samples in this work were recorded using a Bio-Rad FTS-135 spectrophotometer. The samples were scanned from 4000 to 500 cm^{-1} with a resolution of 4 cm^{-1}. One hundred and twenty scans were averaged for each spectrum.

X-ray photoelectron spectra (XPS) measurements were performed on a Kratos Axis HSi, employing a monochromatic excitation radiation of Al Kα at 1486.6 eV. The photoelectron take-off angle with respect to the polymer surface was set at 90°. A passing energy of 150 eV was used for the survey spectra and 40 eV for the high resolution scans. All spectra recorded were referenced to the C1s peak with an assigned value of 284.6 eV. The cross-sectional surface of the film was examined. Surface elemental stoichiometries were determined from XPS peak area ratios, corrected with the experimentally determined sensitivity factors, and were reliable to within ±10%. The elemental sensitivity factors were determined using stable binary compounds of well-established stoichiometries. In curve fitting, the line width (full width at half maximum, or FWHM) for the Gaussian peaks was

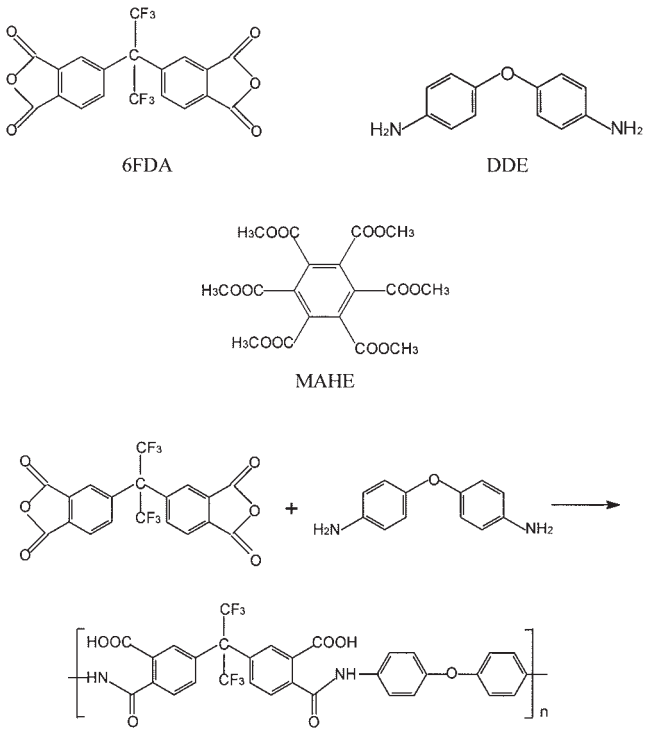

Figure 1 Schematic formulae of monomers and the poly(amic acid) formation formula.

maintained constant for all components in the spectrum of a particular sample.

Storage modulus and loss modulus were measured with a TMA 2940 Thermomechanical Analyzer (TA Instruments) at a ramp rate of 3°C min^{-1} and a frequency of 1 Hz. The samples were heated from ambient to 400°C.

Thermal stability and weight loss behavior were measured using a Setaram Labsys TG/DTA system. The samples (~10 mg) were heated from ambient to 900°C with a heating rate of 10°C min^{-1} in a nitrogen atmosphere and the thermogravimetry analysis (TGA)/differential thermogravimetry (DTG) analysis curves were recorded.

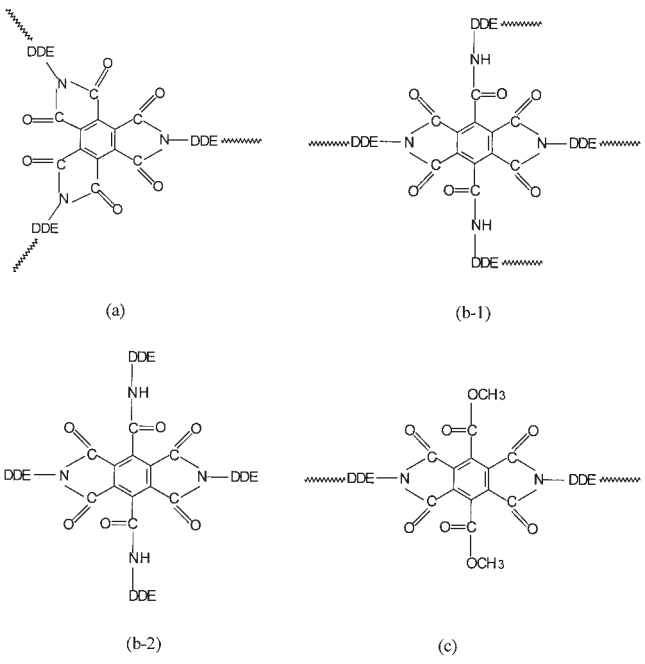

Figure 2 The possible molecular structures in MAP.

RESULTS AND DISCUSSION

XPS study of MAP

MAP is not made up with a uniform molecular structure.[15] In fact, there may exist different types polymers and oligomers (Fig. 2). We can obtain the elemental quantification from XPS which can be correlated to the structures. The possible molecular structures that may result when MAHE and DDE react are shown as (a), (b-1), (b-2), and (c) in Figure 2. The element molar ratios from calculation and XPS experimental results are listed in Table I.

From the calculated and experimental molar ratios of [C]/[O], [C]/[N], and [O]/[N], we can see that it is reasonable to assume that all four polymers indicated in Figure 2 coexist in the MAP system. We expect that structure (a) is the predominant. However, NMR spectra[15] indicated the presence of small amounts of amide and ester, suggesting the presence of (b-1) and (c). The [C]/[O] molar ratio of (c) confirms that this structure does exist in MAP (Table I); furthermore, it contributes significantly to the entire system since this structure is the only one that has a lower [C]/[O] molar ratio (2.89/1) than the experimental value (3.15/1). The existence of structure (c) is also confirmed by the [O]/[N] molar ratio of 4.5/1, which is the only one larger than the experimental value of 2.68/1. In addition, we can also confirm the existence of structure (b-2) from the [C]/[N] molar ratio. Structure (b-2) also indicates the low molecular weight constituent of MAP, which is probably reflected in the experimental observation that MAP is not able to form a stable film. The residual ester group in structure (c) and amine group in structure (b-2) can be explained by the steric hindrance of MAHE and the relatively low reactivity of ester group. Therefore, we may conclude that MAP

TABLE I
Element Molar Ratios from Calculation and XPS

Element molar ratios	Possible molecular structures				XPS
	(a)	(b-1)	(b-2)	(c)	
[C]/[O]	4/1	4.5/1	6/1	2.89/1	3.15/1
[C]/[N]	10/1	9/1	7.5/1	13/1	8.44/1
[O]/[N]	2.5/1	2/1	1.25/1	4.5/1	2.68/1

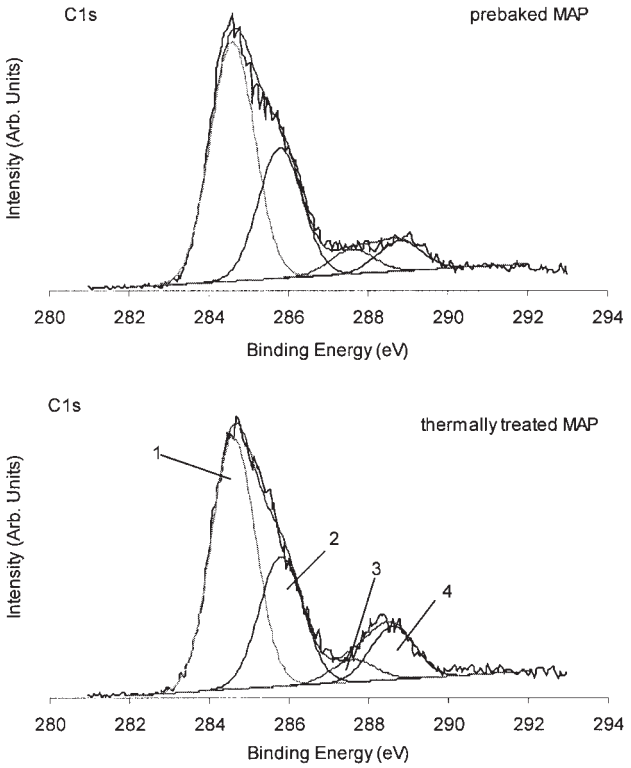

Figure 3 XPS C1s core-level spectra of prebaked and thermally treated MAP.

by itself is composite system, which is composed of different polymers and oligomers.

The C1s core-level spectra of the precursor and thermally treated MAP are shown in Figure 3 and the intensities of XPS peak components corresponding to the functional groups are listed in Table II. The peak labeled 3 is ascribed to the amide carbon, which may not have been converted to imide because of steric hindrance. Comparing peaks 3 and 4, the area for peak 4 is larger than that for 3 in the case of the thermally treated MAP, while the areas are about the same for the precursor. This is evidence that amide is converted to imide during imidization. Since the imide carbon —CO—N— and the ester carbon —COOR appear at

TABLE II
The Intensity of XPS Peak Components of Thermally Treated MAP Corresponding to Functional Groups

Assigned functional groups	Binding energy (ev)	Peak label	Area
Phenyl carbon, *C*—H or C—C in MAHE and DDE	284.6	1	753.501
C—O—C in DDE or *C*—N	285.8	2	388.7556
Amide carbon —CO—NH—	287.6	3	66.71792
Imide carbon —CO—N— or residual —COOR	288.6	4	159.658

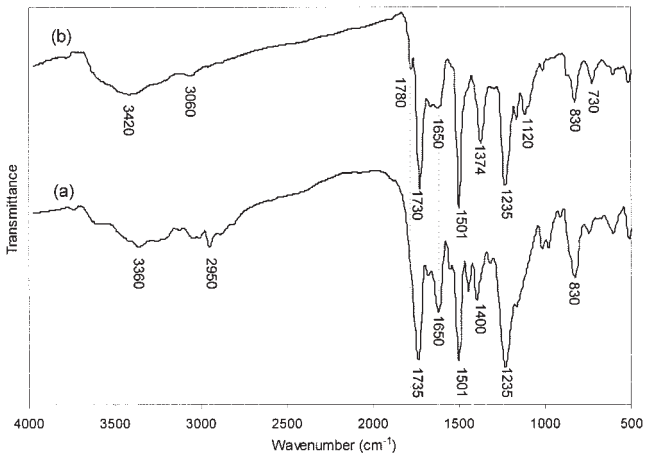

Figure 4 FTIR spectra for MAP: (a) prebaked; (b) thermally treated.

almost the same position, it is not possible to ascertain the extent to which the alkyl ester group has been converted to imide and amide. However, we can differentiate the amide carbon —CO—NH— from imide and ester carbons. They appear at binding energies of 287.6 and 288.6 eV, corresponding to peaks 3 and 4 in Figure 3. Since the alkyl ester group in MAHE monomer can only change to amide or subsequently to the imide group, or remain as ester, we can estimate the amide content in the polymer from the ratio of area of peak 3 to the total area of peak 3 and 4. Thus, we conclude that nearly 30% of the ester carbonyl group in the starting material remains as amide carbonyl group in the final polymer. This is in good agreement with our analysis of the possible structures as shown in Figure 2, since structures (b-1) and (b-2) contain amide groups that take up exactly 1/3 of the original ester carbonyl group.

FTIR study of MAP

The FTIR spectra of the untreated and thermally treated MAP are shown in Figure 4. The two sharp bands near 1780 and 1725 cm^{-1} are characteristic of cyclic imide,[17] and have been ascribed to symmetric and asymmetric imide carbonyl stretching vibrations.[18] The imidization reaction was monitored by following the appearance of these two bands together with bands at 1370 cm^{-1} (C—N stretching) and 730 cm^{-1} (deformation of imide ring).[19–22] As seen in Figure 4, curve (b), peaks at 1780, 1374, 1120, and 730 cm^{-1} confirm that imidization occurs during thermal treatment. Additionally, the disappearance of 1400 cm^{-1} (C—N—C) from spectrum (a) and the weakness of 1650 cm^{-1} (Amide C═O stretching) in spectrum (b) also indicate the conversion from amide to imide.

Both curve (a) and curve (b) show a broad peak assigned to amide N—H stretching near 3400 cm^{-1}

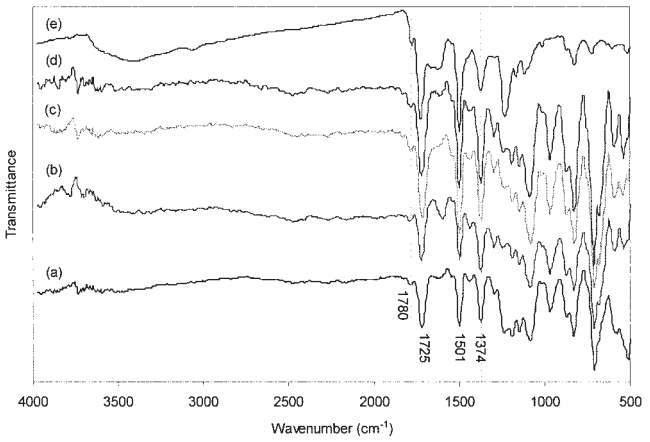

Figure 5 FTIR spectra for 6FDA-DDE, MAP, and 6FBL systems: (a) 6FDA-DDE; (b) 6FBL-5; (c) 6FBL-10; (d) 6FBL-25; (e) MAP.

and a weak peak assigned[23] to methyl C—H asymmetric stretching near 3000 cm^{-1}. The appearance of these two peaks provides corroborating evidence to our conclusion that MAP comprises species with slightly different structures.

Thermally treated MAP shows narrower and smoother peaks than does untreated MAP from 2800 to 3700 cm^{-1}. Also, both the N—H stretching and C—H asymmetric stretching bands display substantial displacements to higher frequencies after thermal treatment, while there is no change in the position of other bands, for example, the aromatic ring at 830 and 1501 cm^{-1} and the aromatic ether[24] at 1235 cm^{-1}. This can be attributed to the imidization reaction and the disappearance or weakness of hydrogen bonding.[25,26]

Linear-network polymer blends (6FBL)

The FTIR spectra of thermally treated 6FDA–DDE, MAP, and 6FBL systems are shown in Figure 5. The 6FBL systems present similar spectra for various network contents. The typical sharp bands near 1780 and 1725 cm^{-1} and absorption at 1374 and 730 cm^{-1} confirm the occurrence of imidization. The N—H stretching (3400 cm^{-1}) and C—H asymmetric stretching (3000 cm^{-1}) bands which appear in MAP cannot be found in either 6FDA–DDE or 6FBL. This indicates the completeness of imidization for 6FDA–DDE and 6FBL. Also, it suggests that the amount of residual amide and methyl species in 6FBL is negligible.

The T_g as obtained from dynamic mechanical analysis (DMA) is an indication of the extent of miscibility in polymer blends. The tan δ versus temperature plots of 6FBL (Fig. 6) show only one relaxation peak for each curve (viz., the α transition), suggesting that the constituents of the blends may be miscible.[27] DMA data of MAP could not be acquired because of its inability to form a stable film. The flat β transition at the vicinity of 150°C results from the secondary relaxations ascribed to side-groups or limited local motions of the chain backbone in the glassy state.[28] The T_g increases with MAP content up to 5% and decreases for higher MAP content. A similar phenomenon has been reported by Barral et al.[29] in diglycidyl ether of bisphenol A epoxy and poly (ether imide) blend systems. The increase in T_g can be ascribed to crosslinks,[30] whereby the mobility of chain segments is reduced. On the other hand, the steric hindrance in MAHE which may result in the formation of low molecular weight components in MAP (Fig. 2) may lead to the latter functioning as a plasticizer, which would decrease the T_g of the blends at higher content. In addition, compared to the 6FDA–DDE homopolymer, tan δ of the T_g relaxation for the blends is broad and exhibits slight decrease in intensity, where 6FBL-5 and 6FBL-8 show the largest change. The decrease in intensity of the relaxation peak may be caused by crosslinking and the differences in the decrease may be attributed to differences in the extent of crosslinking, indicating that a higher extent of crosslinking may have led to the decrease in intensity of the relaxation peak. MAP indicating that a higher extent of crosslinking may have led to the decrease in intensity of the relaxation peak. The broad tan δ transitions suggest inhomogeneities in the local crosslink density.[31,32]

The storage moduli of the blends undergo a sharp and rapid decline at the T_g (Fig. 7). All the blends possess higher moduli than that observed for 6FDA–DDE. The modulus increases with MAP content up to a value of 5% and decreases for samples with higher MAP content and conforms to the effect of MAP observed previously.[14] The storage modulus follows the same trend as that of T_g and may be explained by the difference in crosslink density. MAP could function as a crosslinking agent that induces the formation of a network such that the T_g and the storage moduli of the

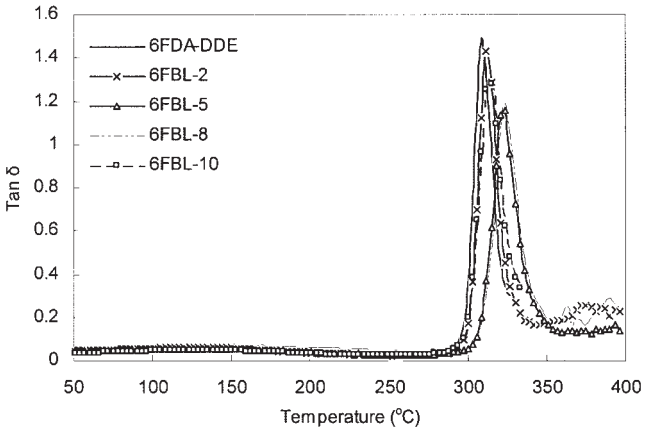

Figure 6 DMA tan δ curves for 6FDA-DDE and 6FBL systems.

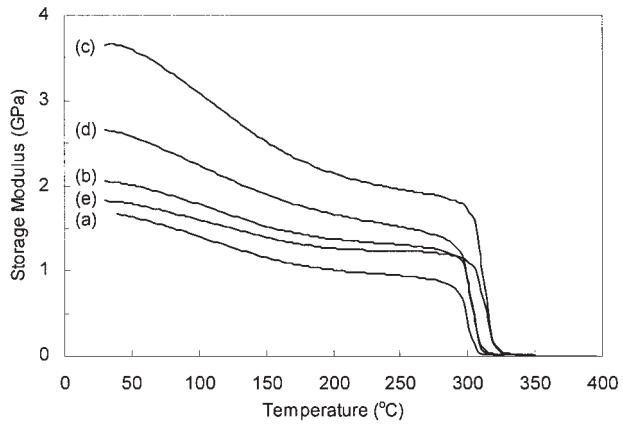

Figure 7 DMA storage modulus curves for 6FDA-DDE and 6FBL systems: (a) 6FDA-DDE; (b) 6FBL-2; (c) 6FBL-5; (d) 6FBL-8; (e) 6FBL-10.

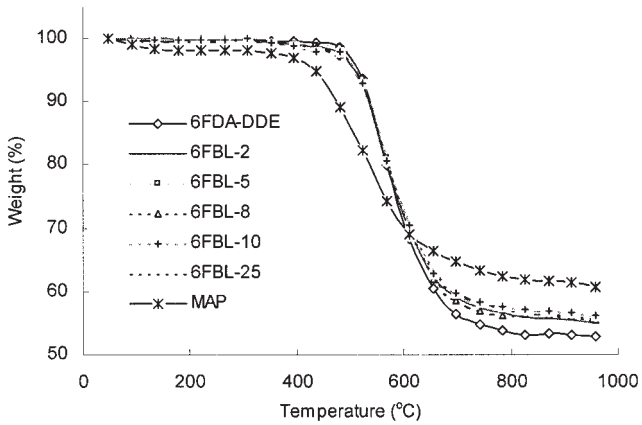

Figure 9 TGA curves for 6FDA-DDE, MAP, and 6FBL systems.

blends are increased for low MAP; MAP could also function as a plasticizer at high MAP content because of its low molecular weight so that it decreases the T_g and storage moduli of the blends.

From the DTG curves for 6FBL (Fig. 8), it can be seen that MAP exhibits two distinct peaks while 6FDA–DDE and 6FBL possess only one peak each. This indicates that there is only one maximum rate of decomposition for the latter materials. Based on our earlier inferences on the composition of MAP, the peak at the lower temperature (480°C) may originate from amide species and the peak at 570°C from the imide. The DTG peak of amide species is a little higher than that reported for PA-6 at 440°C.[33] The negligible methyl ester residue does not show a peak. The peaks for 6FDA–DDE and 6FBL appear at 570°C. The intensity decreases greatly after MAP is introduced into 6FDA–DDE. That is, the rate of weight change is lowered and the weight retention capability at elevated temperature—-which is highly desired for high-temperature applications[34]—-is improved. The negligible amount of amide species in the 6FBL systems may account for the absence of DTG peak around 480°C.

From the TGA curves (Fig. 9), it is evident that MAP decomposes over a wide temperature range with the onset of decomposition occurring at a temperature much lower than that for 6FDA–DDE and 6FBL. However, the weight retention capability follows the order: MAP > 6FBL > 6FDA–DDE and there is little difference among the 6FBL systems containing different MAP contents. As observed earlier, the increase of the residue may be the result of the formation of a carbonized structure promoted by the network structure of MAP.[13,14]

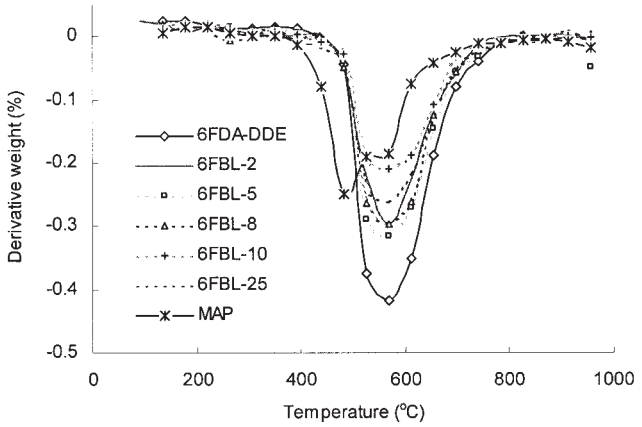

Figure 8 DTG curves for 6FDA-DDE, MAP, and 6FBL systems.

Linear-network copolymers (6FCO)

The 6FCO copolymers present spectra similar to each other, as shown in curve (b), (c), and (d) of Figure 10. For the copolymers, the typical sharp bands near 1780

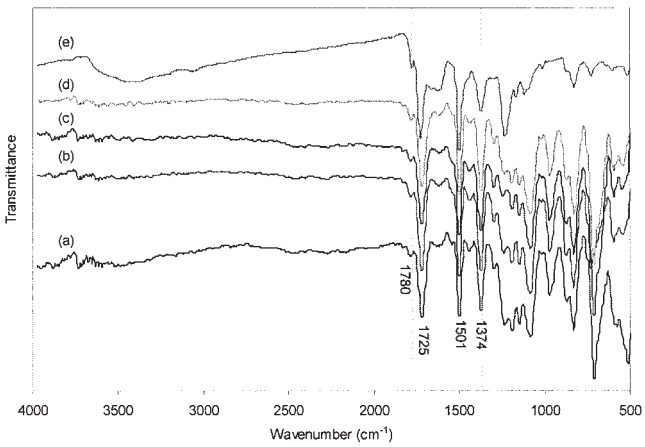

Figure 10 FTIR spectra for 6FDA-DDE, MAP, and 6FCO systems: (a) 6FDA-DDE; (b) 6FCO-5; (c) 6FCO-10; (d) 6FCO-25; (e) MAP.

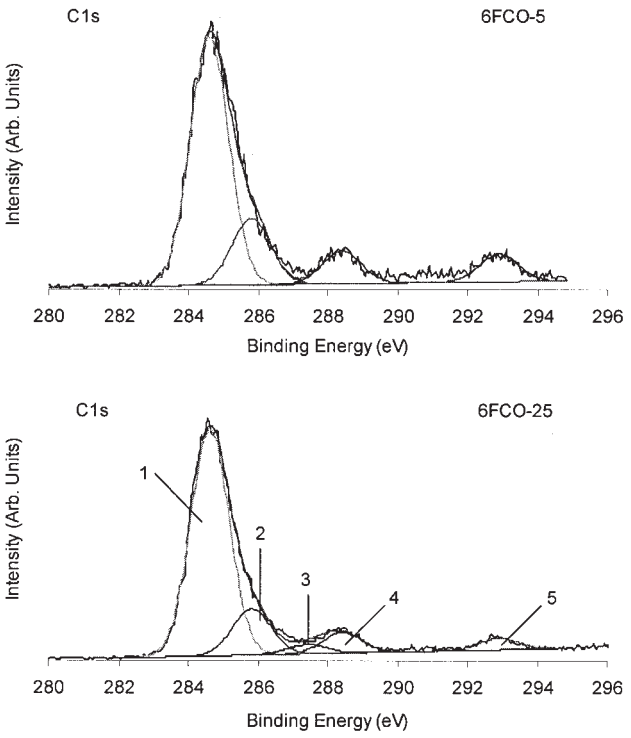

Figure 11 XPS C1s core-level spectra of thermally treated 6FCO-5 and 6FCO-25.

and 1725 cm^{-1}, plus absorption at 1374 and 730 cm^{-1} confirm the occurrence of imidization reaction.[17–22] N—H stretching (3400 cm^{-1}) and C—H asymmetric stretching (3000 cm^{-1}) bands are not observed in either 6FDA–DDE or 6FCO, indicating completeness of imidization. The residual amide and methyl species may not be in sufficient quantities to be detected by FTIR.

The C1s core-level spectra of thermally treated 6FCO-5 and 6FCO-25 are shown in Figure 11. Four peak components are observed for 6FCO-5, having BEs at 284.6 eV for the C—H and C—C, 285.8 eV for the C—O and C—N, 288.6 eV for the —$COOCH_3$ and N(C═O_2), and 292.9 eV for the —CF_3. The spectrum for 6FCO-25 contains an additional peak at 287.6 eV for the O═C—NH species, which has also been found in the XPS study of MAP. Occurrence of this peak for 6FCO-25 indicates the presence of residual amide for this composition.

The tan δ versus temperature plots of the 6FCO systems measured by DMA show a maximum for the T_g of 6FCO near 8% MAP content (Fig. 12). The trend of T_g variation is similar to that of 6FBL. Again, the increase of T_g is ascribed to crosslinking,[30] as in the blend systems. Upon comparing the T_g values for 6FBL and 6FCO, it can be seen that copolymers possess higher T_g value for the same MAP content. The copolymers may possess comparatively better crosslinking structures and more crosslinks.

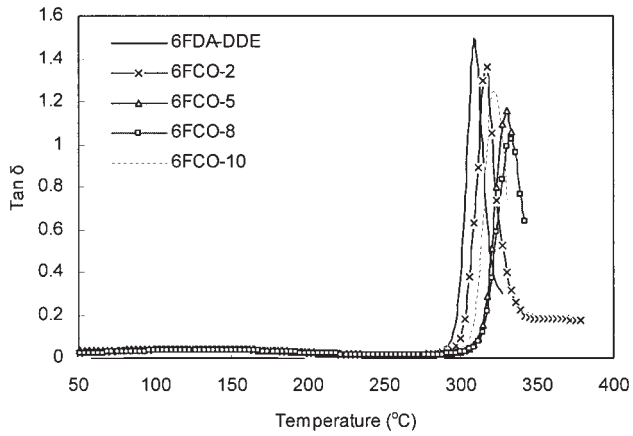

Figure 12 DMA tan δ curves for 6FDA-DDE and 6FCO systems.

As observed for the blends, copolymers possess higher storage moduli than does the 6FDA–DDE homopolymer (Fig. 13). The modulus has a maximum value at 8% MAP content and follows the same trend as that of the T_g. In addition, the increase in strength of copolymers over the linear polyimide is even greater than the increase observed for blend systems. The similar difference noted in PMDA–DDE systems was ascribed to the difference in the nature of the reinforcement between blends and copolymers. The reinforcement is more likely to be physical than chemical in the blends, while the reverse is more likely in copolymers.[15] Correlating the dynamic mechanical properties of blend and copolyimide systems, it is found that both MAP and MAHE improve the storage modulus of the film.

The DTG peaks of the 6FCO copolymers are in the vicinity of 560°C and the single peak indicates that there is only one decomposition (Fig. 14). Compared to 6FDA–DDE homopolyimide, the peak intensities of

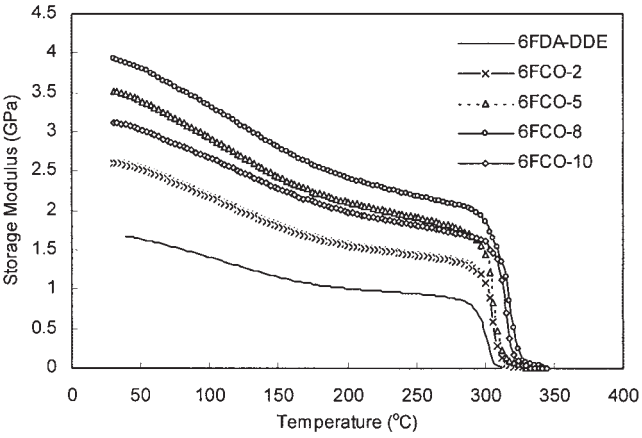

Figure 13 DMA storage modulus curves for 6FDA-DDE and 6FCO systems.

6FCO copolymers are lower. The TGA curves are shown in Figure 15. Similar to blend systems, the onset decomposition of MAP is at a lower temperature than for the copolymers, but the weight retention capability of MAP is superior. The weight retention capability follows the order: MAP > 6FCO-8 > 6FCO-5 > 6FCO-2 > 6FCO-10 > 6FDA–DDE. The differences among the copolymers suggest the higher degree of crosslinking and greater effectiveness of the crosslinked structures in forming a carbonized structure upon decomposition.

CONCLUSIONS

It is confirmed that MAP is composed of different polymers and oligomers, with amide and ester species coexisting with imide species even in the imidized form of MAP. Nearly 30% of the ester carbonyl group in the starting material remains as amide carbonyl group in the final polymer. After the imidization reaction, the hydrogen bonding becomes weakened or disappears.

The presence of crosslinking agents (MAP and MAHE) improves the storage modulus and increases the T_g of the material. The decreases in intensity of the T_g relaxation in the blend and copolymer systems are attributed to crosslinking while the broad tan δ transitions suggest local inhomogeneities in crosslink density. Compared to the blends, copolymers possess higher T_g values for the same content of the network component. The occurrence of an optimum in the amount of the multifunctional constituent for improving thermal and mechanical properties suggests that there is a trade-off between its crosslinking ability if present in low amounts and its plasticizing effect at higher content. Because of the formation of networks, the rate of weight loss is lowered and the weight retention capability at elevated temperature is improved. The technique of incorporating multifunctional species to form networks is shown to be a good method for improving the desirable properties of polyimide.

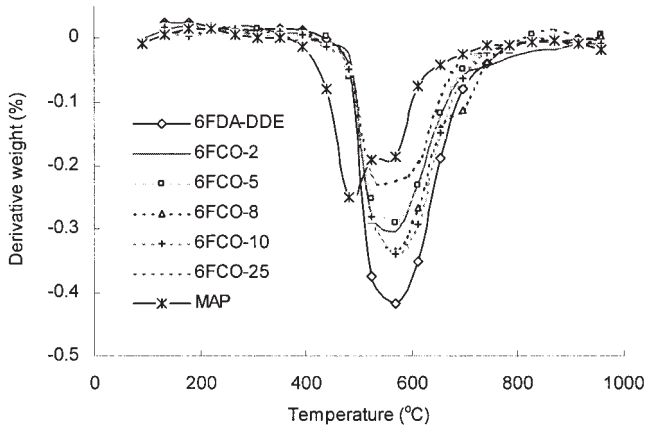

Figure 14 DTG curves for 6FDA-DDE, MAP, and 6FCO systems.

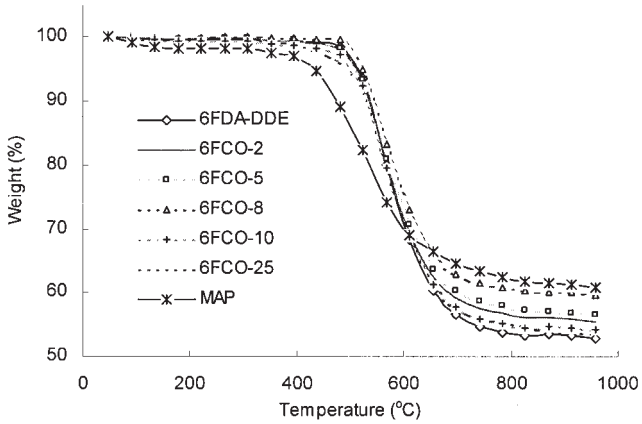

Figure 15 TGA curves for 6FDA-DDE, MAP, and 6FCO systems.

The authors thank Professor Neal Chung and Dr. Pallathadka Pramoda Kumari (IMRE) for the thermomechanical measurements.

References

1. Ghosh, M. K.; Mittal, K. L. In Polyimides: Fundamentals and Applications; Ghosh, M. K., Mittal, K. L., Eds.; Marcel Dekker: New York, 1996.
2. Hamid, S. H.; Atiqullah, M. J Macromol Sci Rev Macromol Chem Phys 1995, C35, 495.
3. Burks, H. D.; St Clair, T. L. J Appl Polym Sci 1985, 30, 2401.
4. Oishi, Y.; Itoya, K.; Kakimoto, M.; Imai, Y. Polym J 1989, 21, 771.
5. Yamamoto, Y.; Kitahashi, M.; Koezuke, H.; Etoh, S. Polym Prepr (Am Chem Soc Div Polym Chem) 1989, 30, 156.
6. Yokota, R.; Horiuchi, R.; Kochi, M.; Soma, H.; Mita, I. J Polym Sci Part C: Polym Lett 1988, 26, 215.
7. Kochi, M.; Uruji, T.; Iizuka, T.; Mita, I. J Polym Sci Part C: Polym Lett 1987, 25, 441.
8. Mita, I.; Kochi, M.; Hasegawa, M.; Iizuka, T.; Soma, H.; Yokota, R.; Horiuchi, R. In Polyimides: Materials, Chemistry and Characterization; Feger, C., Khojasteh, M. M., McGrath, J. E., Eds.; Elsevier Science: Amsterdam, 1989; p 1.
9. Yokota, R.; Horiuchi, R.; Kochi, M.; Takahashi, C.; Soma, H.; Mita, I. In Polyimides: Materials, Chemistry and Characterization; Feger, C., Khojasteh, M. M., McGrath, J. E., Eds.; Elsevier Science: Amsterdam, 1989; p 13.
10. Pater, R. H.; Morgan, C. D. SAMPE J 1988, 24, 25.
11. Takekoshi, T.; Terry, J. M. Polymer 1994, 35, 4874.
12. Földes, E.; Fekete, E.; Karasz, F. E.; Pukánszky, B. Polymer 2000, 41, 975.
13. Nagata, M.; Kiyotsukuri, T.; Moriya, T.; Tsumi, N.; Sakai, W. Polymer 1995, 36, 2657.
14. Wang, J. W.; Srinivasan, M. P.; Ng, S. C. J Mater Chem 1999, 9, 655.
15. Wang, J. W. PhD Thesis, National University of Singapore, 2000.
16. Sasaki, S.; Nishi, S. In Polyimides: Fundamentals and Applications; Ghosh, M. K., Mittal, K. L., Eds.; Marcel Dekker: New York, 1996; p 71.
17. Matsuo, T. Bull Chem Soc Jpn 1964, 37, 1844.

18. Reimschuessel, H. K.; Roldan, L. G.; Sibilia, J. P. J Polym Sci Part A-2: Polym Phys 1968, 6, 559.
19. Snyder, R. W. In Polyimides: Materials, Chemistry and Characterization; Feger, C., Khojasteh, M. M., McGrath, J. E., Eds.; Elsevier Science: Amsterdam, 1989; p 363.
20. Snyder, R. W.; Thomson, B.; Bartges, B.; Czerniawski, D.; Painter, P. C. Macromolecules 1989, 22, 4166.
21. Pryde, C. A. J Polym Sci Part A: Polym Chem 1989, 27, 711.
22. Pryde, C. A. J Polym Sci Part A: Polym Chem 1993, 31, 1045.
23. Silverstein, R. M.; Bassler, G. C.; Morrill, T. C. Spectrometric Identification of Organic Compounds, 3rd ed.; Wiley: New York, 1974.
24. Pramoda, K. P.; Chung, T. S.; Liu, S. L.; Oikawa, H.; Yamaguchi, A. Polym Degrad Stabil 2000, 67, 365.
25. Guerra, G.; Williams, D. J.; Karasz, F. E.; MacKnight, W. J. J Polym Sci Part B: Polym Phys 1988, 26, 301.
26. Guerra, G.; Choe, S.; Williams, D. J.; Karasz, F. E.; MacKnight, W. J. Macromolecules 1988, 21, 231.
27. Chung, T. S.; Herold, F. K. Polym Eng Sci 1991, 31, 1520.
28. McCrum, N. G.; Read, B. E.; Williams, G. Anelastic and Dielectric Effects in Polymeric Solids; Wiley: New York, 1967.
29. Barral, L.; Cano, J.; López, J.; López-Bueno, I.; Nogueira, P.; Ramírez, C.; Torres, A.; Abad, M. J. Thermochim Acta 2000, 344, 137.
30. Ward, I. M. Mechanical Properties of Solid Polymers, 2nd ed.; Wiley: New York, 1983.
31. Gaw, K.; Suzuki, H.; Jikei, M.; Kakimoto, M.; Imai, Y. Macromol Symp 1997, 122, 173.
32. Crawford, D. M.; Escarsega, J. A. Thermochim Acta 2000, 357, 161.
33. Hornsby, P. R.; Wang, J.; Rothon, R.; Jakson, G.; Wilkinson, G.; Cossick, K. Polym Degrad Stabil 1996, 51, 235.
34. Cella, J. A. In Polyimides: Fundamentals and Applications; Ghosh, M. K., Mittal, K. L., Eds.; Marcel Dekker: New York, 1996; p 343.